Thermochimica Acta, 229 (1993) 69–84
Elsevier Science Publishers B.V., Amsterdam

A new method to estimate transition temperatures and heats by peak form analysis [1]

J.E.K. Schawe

Sektion für Kalorimetrie, Universität Ulm, D-89069 Ulm (Germany)

(Received and accepted 4 June 1993)

Abstract

A simple model of heat transfer within a dynamic calorimeter is introduced. On the basis of this model the measured signal of a known thermal event in the sample can be calculated. For this result a method is developed to estimate the true transition temperature and enthalpy from only one heating run. The method is valid on melting peaks with and without a stepwise change of heat capacity. The new method has been experimentally verified for different pure substances. This method can be used as a simple and fast calibration check for a differential scanning calorimeter.

INTRODUCTION

Information about the thermal behaviour of substances can be obtained in dynamic calorimetry by analysis of reaction peaks. According to the type of thermal event, different quantities are of interest, such as the beginning of transition (onset temperature), the end of transition (offset temperature), the heat of fusion (peak area), or the peak form (purity, turnover etc.). In the literature several methods for the estimation of these values have been suggested [1–5]. These methods often need large experimental expense or do not take the dynamic processes into consideration sufficiently.

Dynamic processes are caused by thermal relaxation. This leads to significant differences between the signal of the physical or chemical heat production in the sample and the measured signal. The time consuming heat transfer, both in the measuring instrument and the sample, is the reason for this "smearing" of the measured signal. The measured temperature is thus shifted and the shape of the curve is changed. Mathematical methods of linear response theory are recommended to desmear the measured curves [6]. Use of this method requires linearity and time invariance of the system (sample and measuring instrument). In

[1] Presented at the Tenth Ulm Conference, Ulm, Germany, 17–19 March 1993.

addition the dynamic behaviour (in the form of a Green's function) of the system must be known [7].

Heat conduction is given by a linear differential equation (if α is constant)

$$\frac{\partial^2 T(r,t)}{\partial r^2} = \alpha \frac{\partial T}{\partial t} \tag{1}$$

with $\alpha = (\rho c_p)/\lambda$, ($\rho$ is the density, c_p the specific heat capacity, and λ the thermal conductivity. If the thermal properties of the sample change during the measurement, α is not a constant factor and eqn. (1) is nonlinear [8]; in that case linear response theory is only an approximation. Additional non linearities appear on changes of the symmetry in the DSC twin arrangement during transitions in the sample [9, 10]. It is proved experimentally that, in the case of thermal events with only small changes of sample properties, the linear response theory is practicable within the limits of measuring accuracy [11].

If we have a thermal event that is coupled to a large change of heat flow in the sample (e.g. a melting peak), the effective heating rate of the sample is not equal to the programmed heating rate. This violates the time invariance principle. This effect must be considered at the interpretation of DSC curves [10].

A method of analysis of smeared peaks without the preceding estimation of a Green's function is introduced in this paper. This method, based on a simple model of heat transfer, is experimentally verified for first order phase transitions.

THE MODEL

Algebraic solutions are often preferred to numerical investigations to describe the behaviour of calorimeters and deduce evaluation methods. Relatively simple models are needed to be able to solve with meaningful effort the differential equations which arise. We use a one dimensional model of the differential scanning calorimeter furnace (Fig. 1). On the bottom it is heated with a constant heating rate. The necessary heat flow rate $\Phi_m(t)$ corresponds to the measured signal. The sample is thought to be on the upper end of the heat conducting path. Adiabatic conditions are supposed on this side of the furnace–sample system. Important special cases of this model have previously been calculated [12].

If we change the temperature by a certain heating programme a heat flow rate Φ_s into the sample occurs which describes its behaviour.

The coupling between sample and furnace is thought to be not ideal. The heat transfer is characterized by the heat transfer coefficient k_t. The

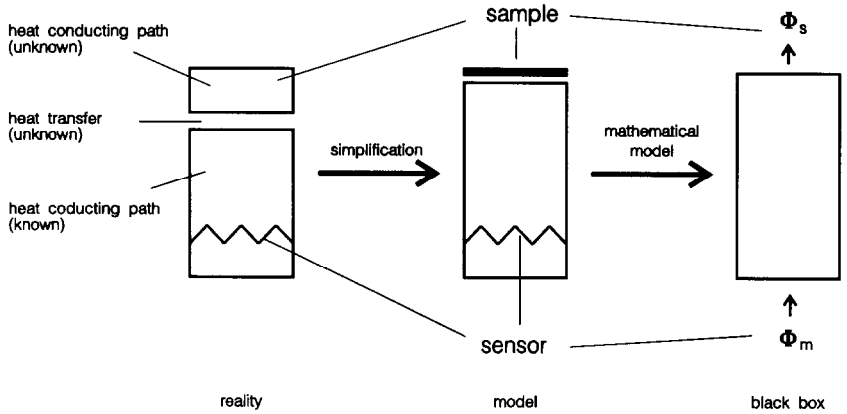

Fig. 1. Simple model of the arrangement of DSC furnace and sample.

thermal conductivity of the furnace is given by the heat transfer coefficient k_f

$$k_f = \frac{l}{A\lambda_f} m_f c_{p,f} \tag{2}$$

where l is a dimension of the furnace, A is the effective cross section area, λ_f is the thermal conductivity coefficient of the furnace material, and m_f, $c_{p,f}$ are the mass and specific heat capacity of furnace respectively.

By analogy to ref. 12 the measured signal at given heat flux into the sample can be calculated as

$$\Phi_m(t) = \frac{\pi}{k} \sum_{n=0}^{\infty} (-1)^n (2n+1) \int_0^t e^{-\frac{(2n+1)^2\pi^2}{4k}(t-t')} \Phi_s(t')\, dt' \tag{3}$$

with $k = k_f + k_t$.

If the thickness of the sample is large in relation to its thermal conductivity, a relatively large temperature profile develops inside the sample. In the one dimensional approximation an isothermal melting front is produced in the sample during the melting process. This effect causes a curvature of the rising edge of the melting peak [12]. In this paper this effect is not considered; in our model the sample is thought to be infinitely thin.

THE IDEAL MELTING PEAK

In the case of linear heating (with heating rate β) of a sample with a heat capacity of $C_p = mc_p$ a constant heat flow rate

$$\Phi = mc_p\beta \tag{4}$$

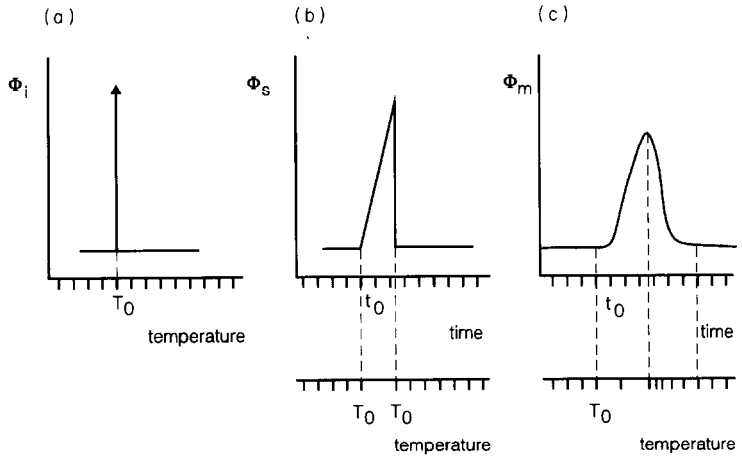

Fig. 2. Ideal sample signal and real measured signal in the case of a first order transition in the sample. (a) Ideal infinite sample heat flow rate, (b) ideal but finite sample heat flow rate (c) real measured heat flow rate.

arises. If at temperature T_0 a first order phase transition takes place in the sample, the total heat of fusion must be put into the sample during a infinitely small time interval. The required heat flux thus has the shape of a Dirac pulse (Fig. 2(a)). In reality the finite power of the heater and heat transfer conditions cause the heat flux into the sample to be limited as well. The sample temperature does not change until the melting process is completed. During that part of measurement the temperature gradient between furnace and sample changes linearly because the furnace is linearly heated and the sample temperature is constant. Hence we find a linear increase of heat flow rate into the sample until the end of transition. The theoretical curve of heat flow into the sample has the shape of a saw tooth triangle (Fig. 2(b)).

Heat relaxation processes cause "smearing" effects, leading to a measured signal that is not in the form of an ideal triangle (Fig. 2(c)).

The shape of the theoretical heat flow rate curve reads (Fig. 2(b))

$$\Phi_s(t) = \begin{cases} at \text{ if } t_0 \leqslant t < t_e \\ 0 \text{ if } (t < t_0) \text{ or } (t \geqslant t_e) \end{cases} \tag{5}$$

The slope a is given by the heat transfer conditions. The integral of the curve (and with it t_e at given slope) is determined by the heat of fusion.

The constant heat flow rate before and after transition due to the heat capacity of the sample (eqn. (4)) is neglected in eqn. (5). It arises only as an additive constant term in the following calculations. For the sake of simplicity t_0 is set at zero. Inserting eqn. (5) into eqn. (3), the measured signal reads

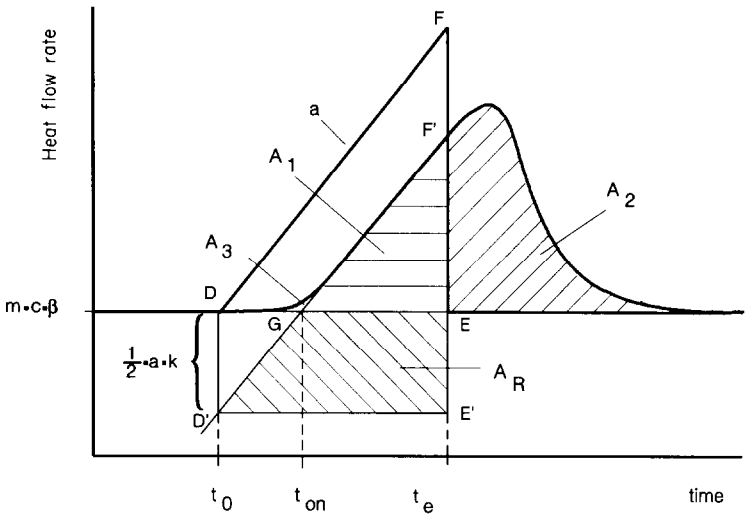

Fig. 3. Schematic presentation of first order transition in the sample and calculated heat flow rate curve due to eqn. (6).

$$\Phi_m(t) = \begin{cases} at - \frac{1}{2}ka + \frac{16}{\pi^3}ka\sum_{n=0}^{\infty}\frac{(-1)^n}{(2n+1)^3}e^{-x_n t} & \text{if } t_0 \leqslant t < t_e \\ \frac{4}{\pi}at_e\sum_{n=0}^{\infty}\frac{(-1)^n}{2n+1}e^{x_n(t_e-t)} \\ -\frac{16}{\pi^3}ka\sum_{n=0}^{\infty}\frac{(-1)^n}{(2n+1)^3}e^{x_n(t_e-t)} & \text{if } t \geqslant t_e \\ +\frac{16}{\pi^3}ka\sum_{n=0}^{\infty}\frac{(-1)^n}{(2n+1)^3}e^{-x_n t} \end{cases} \quad (6)$$

with $x_n = (2n+1)^2\pi^2)/4k$. The heat flow rate into the sample and the corresponding measured signal are shown in Fig. 3.

From eqn. (6) we find the following.

(i) In the region from t_0 to t_e the measured peak is described as a sum of three terms. The first term corresponds to the event in the sample, the other two describe the relaxation processes due to the switching-on. For small times the heat flow rate is zero, at larger times (but below t_e) the slope of the measured peak is nearly the constant a. The second term of the equation describes the shift between t_0 and the experimentally estimated onset temperature t_{on}.

(ii) In the region $t > t_e$ the "switch-off relaxation" is starting. This equation also consists of three terms. The third summand is very small. Both the other terms describe a maximum at a certain $t > t_e$.

In contrast the theoretical signal of the sample is completely characterized by the time t_0, the slope a and the area (heat of fusion Q_{fus}).

Therefore an evaluation method is necessary to obtain these values from the measured curve. Q_{fus} (area) and a (slope) can be estimated relatively easily from the measured curve. The problem is the estimation of the true starting time t_0.

As shown in eqn. (6) the input function Φ_s drops by $0.5ak$ (neglecting the relaxation). Extrapolation of the initial slope of the measured curve to a value $0.5ak$ above the baseline yields t_0 (Fig. 3). Unfortunately k is not known, but from the law of conservation of energy, the triangle D'E'F' must be congruent to the triangle DEF on the one hand and have the same area as the total peak of the smeared signal on the other.

We are able to determine the unknown quantities k, t_e, and t_0 as follows. The areas in Fig. 3 are determined by

$$A_R = \frac{ka(t_e - t_0)}{2} - \frac{(t_{on} - t_0)a}{2} \tag{7}$$

$$A_2 = \int_{t_e}^{\infty} \Phi_m(t)\,dt \tag{8}$$

Inserting eqn. (6) into eqn. (8) and integrating yields

$$A_2 = \tfrac{1}{2}ka(t_e - t_0) - \frac{5}{24}k^2a + \frac{64}{\pi^5}k^2a \sum_{n=0}^{\infty} \frac{(-1)^n}{(2n+5)^5} e^{-x_n(t_e - t_0)} \tag{9}$$

with

$$\sum_{n=0}^{\infty} [(-1)^n/(2n+1)^3] = \frac{\pi^3}{32} \quad \text{and} \quad \sum_{n=0}^{\infty} [(-1)^n/(2n+1)^5] = 5\pi^5/1536.$$

The small relaxation area A_3 at the beginning of the measured peak (Fig. 3) is

$$A_3 = \int_{t_0}^{t_e} (\Phi_m(t) - (at - \tfrac{1}{2}ka))dt - \frac{(t_{on} - t_0)a}{2} \tag{10}$$

Insertion of eqn. (6) and integration yields

$$A_3 = \frac{5}{24}k^2a - \frac{64}{\pi^5}k^2a \sum_{n=0}^{\infty} \frac{(-1)^n}{(2n+5)^5} e^{-x_n(t_e - t_0)} - \frac{(t_{on} - t_0)a}{2} \tag{11}$$

Comparing eqns. (7), (9) and (11) results in

$$A_R = A_2 + A_3 \tag{12}$$

From Fig. 3 we find the validity of

$$\tfrac{1}{2}ka = (t_{on} - t_0)a \tag{13}$$

Paying attention to eqn. (13) and inserting eqn. (7) into eqn. (12) we obtain

$$A_2(t_e) + A_3 = a(t_{on} - t_0)(t_e - t_0) - \frac{a(t_{on} - t_0)^2}{2} \tag{14}$$

The area A_3 between measured curve, baseline, and tangent of the peak can easily be determined from the measured curve. The same is also true for a and t_{on}, whereas A_2 depends on the unknown time t_e.

If we take t_e as known, eqn. (14) can be solved for t_0. To simplify the equation, a transformation of the abscissa is carried out, so that $t_{on} = 0$

$$t_0' = t_0 - t_{on} \tag{15a}$$

and

$$t_e' = t_e - t_{on} \tag{15b}$$

From eqn. (14) we obtain the quadratic equation

$$A_2(t_e) + A_3 = \frac{a}{2} t_0'^2 - a t_e t_0'$$

the solution of which is

$$t_0' = t_e' - \sqrt{t_e'^2 + \frac{2(A_2(t_e) + A_3)}{a}} \tag{16}$$

Now the problem arises of how to estimate t_0 and t_e. The triangle GEF′ with area A_1 is given as

$$A_1 = A - A_3 - A_2(t_e) = \frac{(t_e - t_{on})^2 a}{2} \tag{17}$$

with A being the total area of the melting peak. With the named timescale transformation (eqn. (15)), eqn (17) can be solved

$$t_e' = \sqrt{\frac{(A - A_3 - A_2(t_e))2}{a}} \tag{18}$$

This equation makes an iterative solution possible. Taking the time at peak maximum as starting value, inserting eqn. (18) into eqn. (16) yields

$$t_0' = t_e' - \sqrt{\frac{2A}{a}} \tag{19}$$

We can determine t_0 via eqns. (15) and (19). With

$$T(t) = T_{start} + \beta t \tag{20}$$

we obtain the transition temperature T_0.

To estimate t_0 from measuring curves needs an estimation of slope a which is as accurate as possible.

TRANSITIONS INCLUDING c_p CHANGES

In this section the influence of a c_p change during a transition on the measured signal is investigated.

This type of transition yields baseline changes which restrict the accurate

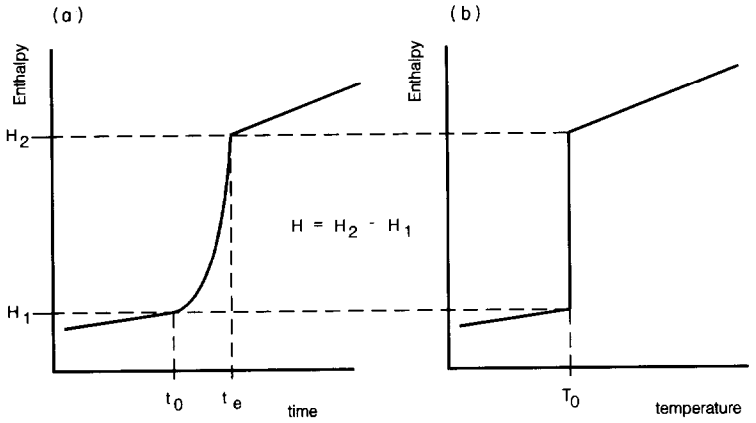

Fig. 4. Enthalpy change of a sample with first order transition and a c_p stepwise change (Fig. 5) depending on (a) time and (b) sample temperature.

determination of both transition temperature and transition heat Q_{fus}. A lot of effort has been made to find the "true" baseline in this case. A detailed comparison of different methods is given in ref. 13. From a physical point of view the determination of transition enthalpy from extrapolation of the enthalpy–temperature function [4] seems to be the best method. However problems occur in practice, because the differential scanning calorimeter measures heat flow rates, not as a function of temperature, but as a function of time, and the proportionality between time and sample temperature is destroyed if a transition occurs [10]. In addition the true transition temperature is not identical with the onset temperature T_{on}.

Without restriction of generality, we shall only discuss the case of increasing heat capacity during transition. The enthalpy–time curve of this case is shown in Fig. 4 and the equivalent heat flow rate into the model sample is shown in Fig. 5. The c_p value jumps at t_e in this model, because

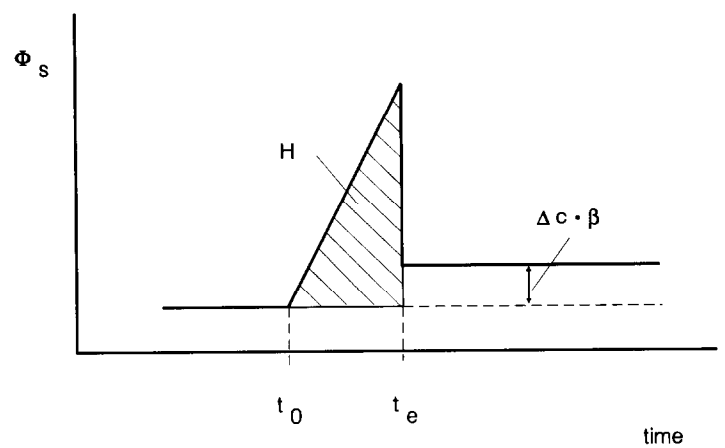

Fig. 5. Ideal heat flow rate into a sample with first order transition and stepwise change of heat capacity.

the enthalpy curve has the new slope starting at that point. By analogy to eqn. (5) the signal of sample reads

$$\Phi_s(t) = \begin{cases} at & \text{if } t_0 \leq t < t_e \\ \Delta C\beta & \text{if } t \geq t_e \end{cases} \tag{21}$$

Insertion of eqn. (21) into eqn. (3) yields the measured signal

$$\Phi_m(t) = \begin{cases} at - \frac{1}{2}ka + \frac{16}{\pi^3}ka \sum_{n=0}^{\infty} \frac{(-1)^n}{(2n+1)^3} e^{-x_n t} & \text{if } t_0 \leq t < t_e \\ \frac{4}{\pi} at_e \sum_{n=0}^{\infty} \frac{(-1)^n}{2n+1} e^{x_n(t_e - t)} & \\ -\frac{16}{\pi^3}ka \sum_{n=0}^{\infty} \frac{(-1)^n}{(2n+1)^3} e^{x_n(t_e - t)} & \\ +\frac{16}{\pi^3}ka \sum_{n=0}^{\infty} \frac{(-1)^n}{(2n+1)^3} e^{-x_n t} & \\ +\Delta C\beta - \frac{4}{\pi}\Delta C\beta \sum_{n=0}^{\infty} \frac{(-1)^n}{2n+1} e^{x_n(t_e - t)} & \end{cases} \quad \text{if } t \geq t_e \tag{22}$$

The corresponding curve is shown in Fig. 6.

A comparison of eqns. (6) and (22) shows that in the region of thermal relaxation two more terms appear in the case of a step change of c_p. These terms describe the curved baseline (HL in Fig. 6) at $t > t_e$, whereas both curves are identical in the first part of the peak ($t_0 < t < t_e$) (straight line GH). The extrapolated straight line KL (up to t_e) can be determined relatively simply from the steady states before and after transition. If the heat of transition is determined from the area between the measured curve

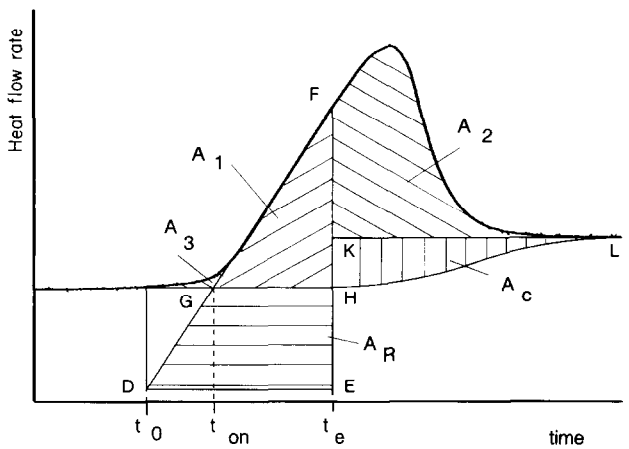

Fig. 6. Schematic presentation of a first order transition with heat capacity change (eqn. (22)).

and these lines, an error is made. This error is equal to the area A_c.

$$A_c = \int_{t_e}^{\infty} \frac{4}{\pi} \Delta C \beta \sum_{n=0}^{\infty} \frac{(-1)^n}{2n+1} e^{x_n(t_e - t)} \, dt \tag{23}$$

Integration yields

$$A_c = \tfrac{1}{2} km \, \Delta c_p \beta \tag{24}$$

It can be seen that A_c is determined by the change of the heat capacity of the sample, and heat transport process. A step change in the sample signal at t_e appears in addition to the melting peak. The last two terms in eqn. (22) describe this step.

If at the beginning of the scanning run the heating rate is switched on or at the end of the measurement the heating rate is switched off, a smilar step in the measured signal arises. Between these switchings, the heat capacity of the sample has changed by ΔC_p. The corresponding curves are shown in Fig. 7. The shape of the curves can be calculated by insertion of

$$\Phi_{s,on}(t) = mc_{p,1}\beta\Theta(t - t_{begin})$$

or

$$\Phi_{s,off}(t) = mc_{p,2}\beta(1 - \Theta(t - t_{end}))$$

into eqn. (3). $c_{p,1}$ and $c_{p,2}$ are the specific heat capacities before and after the transition, respectively, t_{begin} and t_{end} are the times of switching on or off of heating rate and $\Theta(t - t')$ is the "step function" The measured signal in the switching-on region reads

$$\Phi_{m,on}(t > t_{begin}) = mc_{p,1}\beta - \frac{4}{\pi} mc_{p,1}\beta \sum_{n=0}^{\infty} \frac{(-1)^n}{2n+1} e^{-x_n(t - t_{begin})} \tag{25a}$$

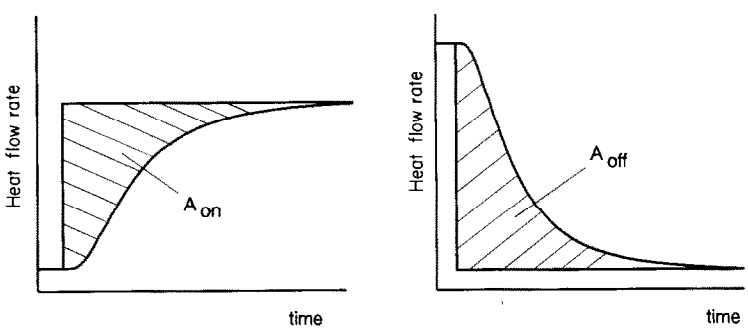

Fig. 7. Relaxation behaviour on switching on and off the heating rate, of a sample with c_p change.

and in the switching-off region

$$\Phi_{m,off}(t > t_{end}) = \frac{4}{\pi} mc_{p,2}\beta \sum_{n=0}^{\infty} \frac{(-1)^n}{2n+1} e^{-x_n(t-t_{end})} \quad (25b)$$

From eqn. (25) the corresponding relaxation areas are

$$A_{on} = -\tfrac{1}{2}kmc_{p,1}\beta \quad (26a)$$

or

$$A_{on} = \tfrac{1}{2}kmc_{p,2}\beta \quad (26b)$$

A comparison of eqns. (24) and (26) yields an approximation of A_c from the areas of relaxation at switching-on and -off, for example

$$A_c = A_{on} + A_{off} \quad (27)$$

We have to emphasize that the formation of the temperature profile inside the furnace is not considered in eqn. (25). However we can show that within the limits of this model the corresponding part of the signal vanishes if we subtract the empty pan baseline [14]. Nevertheless the heat transfer conditions should be kept constant in the sample run and also the baseline run [15], and care should be taken to ensure symmetric conditions [9, 10].

If we determine the peak area A between the measured curve and the extrapolated straight line (KL in Fig. 6) we obtain

$$A = A_1 + A_2 + A_3 \quad (28)$$

and times t_e and t_{on} can also be determined from eqns. (18) and (19). The heat of fusion is then

$$Q_{fus} = A + A_c \quad (29)$$

Thus the relevant peak quantities can be determined accurately without any "baseline construction", as is also the case for transitions with c_p change.

MEASURING RESULTS

The difference between T_{on} and T_0 is caused by smearing of the measured curves by reason of heat transfer. Equation (6) shows that the difference between t_{on} and t_0 is proportional to k and thus depends on the heating rate. If eqn. (20) describes the connection between times and temperatures, the difference $T_{on} - T_0$ depends linearly on heating rate β. This difference vanishes if the heating rate is zero. The onset temperature at heating rate zero can be estimated by means of extrapolation of the onset temperature measured at different heating rates. This method is used for temperature

calibration of a differential scanning calorimeter [1]. If our model presented above is correct, the onset temperature, extrapolated to heating rate zero, should coincide with the temperature T_0 computed according to eqn. (19).

In order to experimentally verify the results from our model, the measured samples should have a good purity, to guarantee sharp melting peaks. Gallium, indium and tin were used for test measurements. The measuring instrument was Perkin-Elmer DSC-II modernized with regard to electronics and computer control. The new design allows any given scanning rate at better signal-to-noise ratio. The sampling rate can be chosen up to 15 values per second [16]. The large sampling rate reduces the numerical error of the peak area estimation at fast scanning rates.

The above named metallic samples were measured at heating rates between 0.5 and 10 K min^{-1}. On the one hand the onset temperatures were determined and on the other hand T_0 was calculated according to eqn. (19). The results are shown in Figs. 8–10. The sample masses in question are mentioned in the legends.

As can be seen, all values of T_0 correspond to the extrapolated onset temperature at heating rate zero T_{ex}. The deviations of T_0 are less than ± 0.1 K min^{-1}. This is in the same range as the error of T_{ex} [17].

In Fig. 8 another value of T_{on} is added, which originates from a first run measurement (at 10 K min^{-1}). (All other results are from at least second run measurements.) This single value is larger than the others (at the same heating rate) because the heat contact between sample and pan is relatively poor at the beginning. In this special case k (in eqn. (6)) is larger than in all other measurements. However T_0 determined by our method from this first run measurement is in excellent agreement with the second run values.

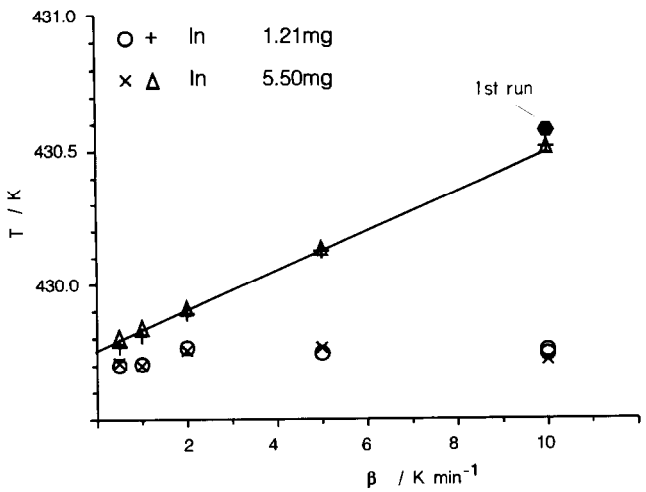

Fig. 8. Dependence of the onset temperature of indium (+, △) on heating rate, together with transition temperature (○, ×) according to eqn. (19).

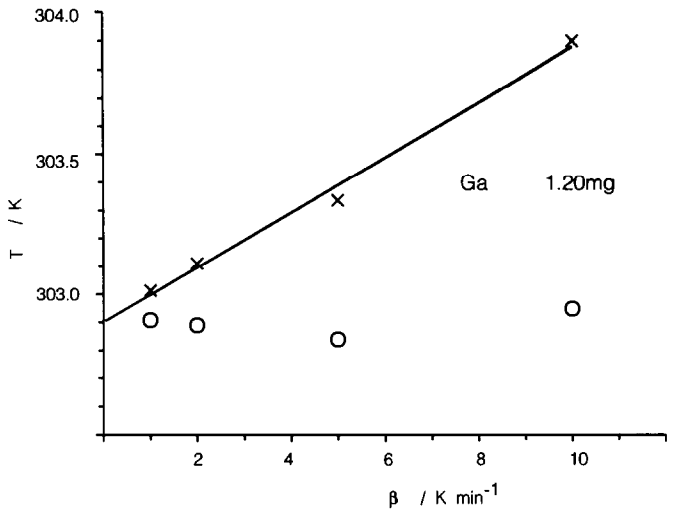

Fig. 9. Dependence of the onset temperature (×) of gallium on heating rate together with transition temperature (○) according to eqn. (19).

One of the tin samples, having a mass of 3.82 mg, did not fuse homogeneously. An isothermal fusion front inside the sample developed. This yielded an expected curvature in the peak slope. In this case the relaxation area A_2 is distinctly too large in the numerical analysis. As a consequence the T_0 values are too small (Fig. 10). This was to be expected because the model calculation presumes a homogeneously melting sample. We can see in the same figure that correct T_0 values are estimated if we use small sample masses.

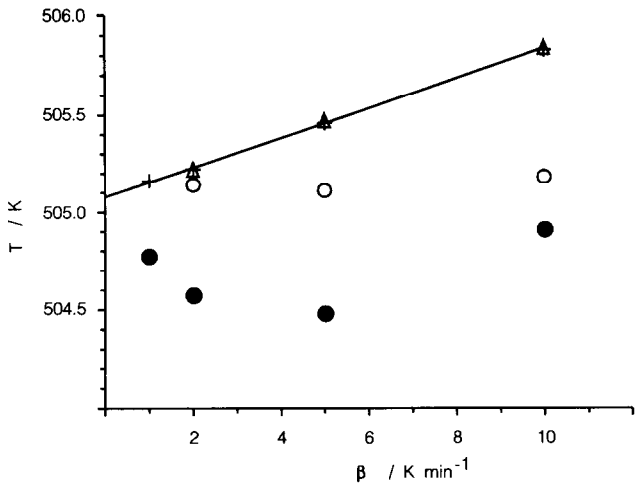

Fig. 10 Dependence of the onset temperature (△, 0.54 mg; +, 3.82 mg) of tin on heating rate together with transition temperature (○, 0.54 mg; ●, 3.82 mg) according to eqn. (19).

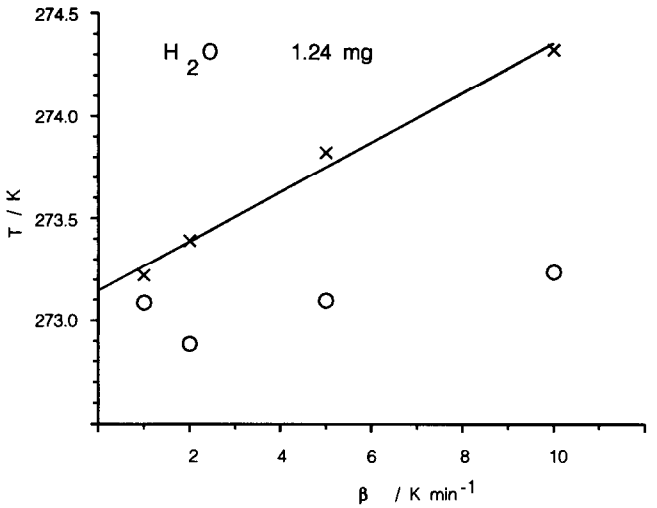

Fig. 11. Dependence of the onset temperature (×) of water on heating rate together with transition temperature (○) according to eqn. (19).

To prove this model of peak analysis in the case of a sample with c_p step change during a transition we measured the melting of water. The results at different heating rates are shown in Fig. 11. The outcome is, in the main, the same as from the metal measurements, but the scatter of T_0 is somewhat larger. When measuring water, one has to take care that no water condensate collects on the inner side of the lid of the pan, otherwise the peak will become broader because of the temperature difference between bottom and lid. This effect presupposes a larger relaxation region of the peak than should occur in reality.

The heats of fusion determined according to eqns. (28) or (29) are presented in Fig. 12. For comparison, Q_{fus} was also determined in the common way, using a straight line as baseline. As can be seen, this method yields heats of fusion which increase with the heating rate. If we determine the peak area with the aid of eqn. (28) (neglecting A_c) the values decrease with heating rate, but to a minor extent. If we include the corrections having regard to the switch-on and switch-off areas (eqn. (29)), we obtain a heat of fusion without any dependence on heating rates. The accuracy of the numerical evaluation of T_0 from measuring peaks with our method depends on the sampling rate of the heat flow rate. In the case of too few measured points in the region of the peak maximum the determination of t_e can be erroneous, in particular for measurements with large heating rate. At a heating rate of 10 K min^{-1} the sampling rate should be at least 4 per second (depending on sample mass and specific heat of fusion in question). Preliminary investigations on this problem showed that the value of the temperature T_0 determined is too small when the sampling rate is too low [14].

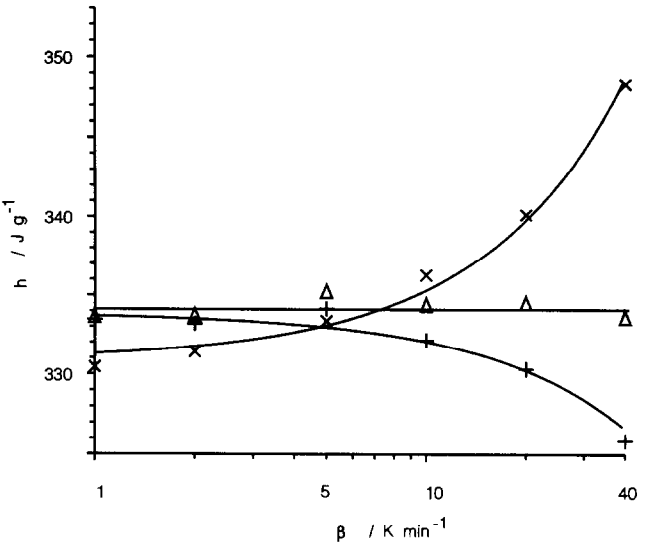

Fig. 12. Specific melting heat of ice as a function of heating rate determined with different methods (×, with straight baseline; +, from areas $A_1 + A_2 + A_3$ (Fig. 6) without A_c; △, from eqn. (29)..

CONCLUSIONS

The result from calculations using an easy model yield a method for determining the temperature and heat of fusion from the measured peaks. The method is based on an easy iterative comparison of partial areas leading to the starting temperature and the peak relaxation area. From this data the true transition temperature, which is lower than the extrapolated onset temperature, can be determined.

Experimental verification yields a good correspondence between transition temperatures determined by our new method and those determined by extrapolation of the onset temperature from different heating rates to heating rate zero. Furthermore, additional smearing effects due to bad contact between sample and pan have no influence on transition temperature; thus in our case, the results from the first run do not differ from the others.

If the transition includes a stepwise change of the heat capacity, the heat of transition can be determined without construction of a non-linear baseline if we have knowledge of the relaxation behaviour of the heat flow on switching the heating rate on and off.

These results show that it is possible to correct the influences of dynamic processes of the calorimeter within the limits of our model.

The procedure presented can be used for quick temperature calibration of the differential scanning calorimeter as only one measurement is needed for determination of the true (unsmeared) transition temperature.

ACKNOWLEDGEMENT

The author thanks Günther W.H. Höhne from the University of Ulm for helpful discussions and support.

REFERENCES

1 G.W.H. Höhne, H.K. Cammenga, W. Eysel, E. Gmelin and W. Hemminger, Thermochim. Acta, 160 (1990) 1.
2 M.J. Richardson, in K.D. Maglic, A. Cezairliyan and V.E. Peletsky (Eds.), Compendium of Thermophysical Property Measurement Methods 2, Plenum Press, New York, 1992, p. 519 ff.
3 W.F. Hemminger and H.K. Cammenga, Methoden der Thermischen Analyse, Springer Verlag, Berlin, 1989.
4 M.J. Richardson, in G. Allen (Ed.), Comprehensive Polymer Science, Vol. 1, Polymer Characterisation, Pergamon Press, Oxford, 1989, p. 868ff.
5 S. Chew, J.R. Griffiths and Z.H. Stachurski, Polymer, 30 (1989) 874.
6 W. Hemminger and G.W.H. Höhne, Calorimetry, Fundamentals and Practice, VCH Verlags-Gesellschaft, Weinheim, 1984.
7 G.W.H. Höhne, J.E.K. Schawe and C. Schick, Thermochim. Acta, 229 (1993) 27.
8 H. Hoff, Can. J. Phys., 68 (1990) 198.
9 J.E.K. Schawe, C. Schick and G.W.H. Höhne, Thermochim. Acta, 229 (1993) 37.
10 J.E.K. Schawe, G.W.H. Höhne and C. Schick, Dynamic behavour of power compensated differential scanning calorimeters, Part 6, in preparation.
11 J.E.K. Schawe, C. Schick and G.W.H. Höhne, Dynamic behaviour of power compensated differential scanning calorimeters, Part 5, in preparation.
12 H. Hoff, Thermochim. Acta, 187 (1991) 293.
13 W.F. Hemminger and S.M. Sarge, J. Therm. Anal. 37 (1991) 1455.
14 J.E.K. Schawe, unpublished results.
15 W. Poeßnecker, Thermochim. Acta, 229 (1993) 97.
16 IfA GmbH, Schillerstraße 18, D-89077 Ulm, Hardware-Handbuch für DSC-2 Modernisierung, Ulm, 1992–1993.
17 G.W.H. Höhne and E. Glöggler, Thermochim. Acta, 151 (1989) 295.